ORIGINAL ARTICLE

Fook Choon Choi · Jianchun Li · Bijan Samali · Keith Crews

Application of modal-based damage detection method to locate and evaluate damage in timber

Keywords: Damage localisation · Severity estimation · Timber · Experimental modal analysis · Modified damage index

---

F.C. Choi · J. Li · B. Samali (✉) · K. Crews

Center for Built Infrastructure Research, Faculty of Engineering, University of Technology Sydney, PO Box 123 Broadway, NSW 2007, Australia

Tel. +61-2-95142023; Fax +61-2-95142868

e-mail: Bijan.Samali@uts.edu.au

Abstract

This paper employs modal-based damage detection algorithms to identify location of defects commonly found in timber and to estimate their severities. In this study, the authors propose modifications to an existing damage detection algorithm for locating and evaluating damage by comparing the modal strain energy before and after damage using the first two flexural modes of vibration. Experimental verification was performed on pin-pin supported timber beams by employing the algorithms with extracted modal parameters using Experimental Modal Analysis (EMA). Single and multiple damage simulating pocket(s) of rot with various severities were inflicted by removing section(s) on timber beam specimens. The proposed damage indicator computed from the first two flexural modes was capable of detecting all damage locations. It was also able to estimate, with reasonable accuracy, the severity of damage in term of loss in sectional moment of inertia. The modified damage index method is in general reliable in detecting location as well as estimating the severity of simulated defects in timber beams.

Introduction

Wood is a versatile building material, as it is abundant, easy to get and renewable. It has gained increased awareness among engineers for the past decade as a viable material to replace concrete and steel construction[1]. Basically, wood is a material 'produced' biologically in the growing tree making it a non-homogeneous material, which contains growth defects in the form of knots, zone with compression wood and oblique fibre orientation[2]. This material is also subjected to damage such as termite attacks and pockets of rot as well as mechanical degradation such as overload and fatigue that inevitably weakens its structural capacity and shortens its service life span. Therefore, developing reliable and efficient nondestructive testing (NDT) techniques for evaluation of wood in structures has become a significant task for engineers.

Various local nondestructive testing (NDT) techniques for wood products have been actively developed to provide accurate information on the properties, performance and condition of wood[3]. However, these techniques are developed mostly to detect faults with damage area to be known a priori, which reduces efficiency and reliability. Thus, global NDT techniques are an essential key in order to make the condition assessment of wood more reliable, and time and cost effective. Modal-based damage detection methods are global NDT techniques that have found application in timber structures lately. However, little research has been reported on timber structures using modal-based methods to detect or to evaluate damage[4-10]. Most of the work to date has been successful in detecting single damage and some for two damage locations computed using either the first or second flexural modes.

On the other hand, progress on modal-based damage detection methods in both laboratories and in the fields in recent years has created opportunities for global NDE of timber structures[4-6]. Among various methods, a method developed by Kim and Stubbs[11] based on changes in modal strain energy as a damage indicator for a structure has been particularly promising. In the literature, this method is often referred to as the damage index method. The method was intended for a wide range of applications to structural systems. Recently, published studies have demonstrated the use of the damage index method to localise and estimate the severity of damage within a structure using a limited number of modal parameters for steel plate girder and other highway bridges.

This paper reports on experimental investigations on timber beams using experimental modal analysis (EMA) to extract the required modal parameters which will then be used for computing the damage index and hence detecting the damage. A modified damage detection algorithm was used to locate and evaluate various damage scenarios in the experimental work. A laboratory investigation was conducted on timber beams with damage inflicted under various damage scenarios using modal tests. The modal parameters obtained from the undamaged and damaged state of the test beam were used in the computation of modal strain energy. A statistical approach was also utilised to detect location of damage. A mode shape reconstruction technique, namely cubic spline interpolation, was used to enhance the capability of the damage detection algorithm with limited number of sensors.

Materials and methods

Materials

Two timber beams of grade MGP12 were used in the experimental work as undamaged beams with their moisture content estimated to be about 7-8%. The beams were of treated radiata pine sawn timber measuring nominal dimensions of 45mm by 90mm (width x height) in cross section with a span length of 4,500mm. A specially designed support system was used to provide a well-defined boundary condition that is very close to a pin-pin support.

Inflicted damage

The goal of this study was to detect defects typically found in timbers. It is aimed to locate damage (single and multiple damage) and evaluate the damage severity in timber beams. The list of cases with various damage inflicted in the timber beams are described in Table 1. All damage scenarios consist of a rectangular opening from the soffit of the beam, located at 2/8, midspan (4/8) and 6/8 of the span length to simulate pockets of rot, which usually starts from the top surface. In this paper and the discussions that follow, L, M and S will be used to denote ‘light’, ‘medium’ and ‘severe’ damage, respectively. All inflicted damage are 1% of the total span length (45mm) and consist of 10%, 30% and 50% of the beam depth, designated as damage cases L, M and S, respectively as shown in Table 1. The 10%, 30% and 50% of the beam depth cut in cross section are corresponding to 27.1%, 65.7% and 87.5% of loss of sectional “I” (moment of inertia), respectively.

Frequency response function (FRF)

The basic concepts of signal analysis starts with the Fourier transform of a continuous signal, which according to J.B. Fourier (1822): “*any real time signal x(t) is a* *superposition of sine waves with their frequency f, their amplitude A and phase angle ϕ'*. The fast Fourier transform (FFT) has made possible conversion of time series data to frequency data without losing any information theoretically. In frequency domain, the input function $f(\omega)$ with respect to frequency ω is obtained from the force applied to the beam with a modal hammer and the output function $g(\omega)$ is obtained from the response of the structure measured by the accelerometers attached to the system. By dividing the frequency function of the input by that of the output as shown in Eq. (1), the frequency response function, FRF or $H(\omega)$ is obtained for each point on the system.

$$H(\omega) = \frac{g(\omega)}{f(\omega)} \tag{1}$$

Experimental Modal Analysis (EMA)

The EMA procedure and instrumentation layout used for the investigation is shown in Fig. 1. The EMA provides natural frequencies, dampings (not discussed in this paper) and corresponding mode shapes. The modal testing, as part of the EMA used in this study, employs an impact hammer to excite the test sample at a strategic location and measuring the acceleration response. Nine accelerometers were used to measure the acceleration response of the beam, which is deemed sufficient number of points along the span so that the mode shapes can be accurately reconstructed using interpolation techniques. One of the accelerometers was used as the driving point measurement, so that the experimental mode shapes could be mass normalised. Each accelerometer was attached onto a small steel plate using magnetic base and secured onto the top of the beams. The accelerometers were located at 1/8 intervals of the span length starting from one end support of the beam to the other end as shown in Fig. 1. The impact location, at 3/4 of the span length, was selected so that more modes can be excited, simultaneously.

The HP VXI with LMS general acquisition monitor was used to record the dynamic response at 10,000 Hz sampling rate for 8,192 data points. LMS frequency domain direct measurement curve-fitting technique was used to obtain the modal frequencies and mode shapes from the measured FRFs. Using the EMA, five vibration modes, with a frequency bandwidth ranging from10Hz to 200 Hz, were captured. However in this paper, only the first two flexural modes were needed. From the nine-point experimental mode shape, a new mode shape vector with 41 points can be reconstructed using cubic spline interpolation technique. The reconstructed mode shape increases reliability and accuracy of damage detection when it is used in damage detection algorithms.

Damage detection algorithms

In this investigation, the damage index method developed by Kim and Stubbs[11] was adopted and modified (named as modified damage index (MDI)) to detect the inflicted damage. The MDI pertaining to damage localisation is based on the relative differences in modal strain energy between an undamaged structure and that of the damaged structure. The modal strain energy utilises derivatives of mode shape, i.e. mode shape curvature, and the algorithm used to calculate the damage index for the *j*th element and the *i*th mode, β_{ij}, is given below.

$$\beta_{ij} = \frac{\int_j \left\{\phi_i^{//*}(x)\right\}^2 dx \int_0^L \left\{\phi_i^{//}(x)\right\}^2 dx}{\int_j \left\{\phi_i^{//}(x)\right\}^2 dx \int_0^L \left\{\phi_i^{//*}(x)\right\}^2 dx} \tag{2}$$

In Eq. (2), the terms $\phi_i''(x)$ or $\phi_i''^*(x)$ are normalised mode shape curvature coordinates of a one-dimensional system, which are normalised with respect to the maximum value of the corresponding mode, corresponding to mode *i* for a beam structure. The asterisk denotes the damage cases. For the original damage index method, although mode shape vectors have been mass normalised, the mode shape curvatures used for the damage index calculation are not normalised. Values of mode shape curvature are dependant on the shapes of each individual mode shape. Instead of reflecting the changes in the curvature due to damage, the summation of non-normalised mode shape curvatures will distort the damage index in favour of higher modes, which results in false damage identifications. The modified damage index method introduced above overcomes the problem by normalising mode shape curvatures with respect to the maximum norm of each mode shape curvature. To account for all available modes, NM, the damage indicator value for a single element *j* is given as

$$\beta_j = \frac{\sum_{i=1}^{NM} Num_{ij}}{\sum_{i=1}^{NM} Denom_{ij}} \tag{3}$$

where NUM_{ij} = numerator of β_{ij} and $DENOM_{ij}$= denominator of β_{ij} in Eq. (2), respectively. Transforming the damage indicator values into the standard normal space, normalised damage index Z_j is obtained:

$$Z_j = \frac{\beta_j - \mu_{\beta j}}{\sigma_{\beta j}} \tag{4}$$

where $\mu_{\beta j}$ and $\sigma_{\beta j}$ are the mean and standard deviation of β_j values for all j elements, respectively. A judgment based threshold value is selected and used to determine which of the j elements are possibly damaged which in real applications is left to the user to define based on what level of confidence is required for localisation of damage within the structure.

The severity of damage in the jth member is estimated using the expression as follows,

$$\alpha_j = 1 - \frac{1}{\beta_j} \tag{5}$$

where α_j = severity estimator.

The effectiveness of Modified Damage Index (MDI) method, introduced above, is closely related to the number of elements of the structure or components. The number of elements to be used by damage detection is dictated by the number of sensors used for the measurement. In order to produce reliable and accurate results, a relatively large number of sensors are required to produce the fine coordinates of the mode shapes. In the numerical simulation, the coordinates can be controlled by mesh density. However, in the field applications or experimental testing, the evaluation of the coordinates of the mode shape vectors is limited by the number of sensors used in the testing which is often far less than what the damage detection requires. To overcome this limitation, a few techniques for reconstructing mode shapes to increase the number of coordinates are proposed. In this paper, cubic spline interpolation technique was used for reconstruction of the mode shapes from experimental testing. The measured mode shape coordinates can be interpolated to generate mode shape vectors of greater length.

Results and Discussion

In the following results, all damage localisation indices for each of the damage cases are plotted against the beam span length. In principle, any location with the index value *Zj* larger than zero (the probability-based criterion for damage detection) is considered as damage existing at that location. For the estimation of damage severity, the graphs are presented in terms of percentage of loss in “I” (sectional moment of inertia). In this case, a weighting coefficient was applied to adjust the severity of damage based on the assumption that the experimental data was polluted with 20-30% noise. The actual damage locations are indicated with dashed line in all figures.

Localisation of damage

The results of applying the Modified Damage Index (MDI) method to compute single damage cases using the first two flexural modes are illustrated in Fig. 2. For single damage cases 1 to 3, the MDI is able to indicate accurately the location of damage at position 2.25m with few false positives (indication of false damage locations) at position 3.375m and near the supports. It is quite clear that as the severity of damage ascends the damage index increases accordingly, having values of 1.00, 3.55 and 4.05, for light, medium and severe damage, respectively. The noted trend is consistent with the results presented by Hu and Afzal[9]. The damage index is able to qualitatively estimate the severity of damage judging from the probability of existence of damage. However, the damage localisation algorithm was not capable of estimating the extent of damage.

Fig. 3 depicts the damage scenarios of two damage locations positioned at 2.25m and 3.375m detected with MDI. The severe damage for damage cases 4, 5 and 6 is precisely identified by the damage indicator. This also applies to the damage at position 3.375m except for light damage of damage case 4. It is clear that the method is capable of detecting damage in dual damage scenarios, but may miss out light damage that appear together with severe damage. This is due to light damage altering slightly the mode shape and its derivatives, which may have been overshadowed by other more severe scenarios.

For three damage location scenarios in damage cases 7 to 9, the damage localisation results are illustrated in Fig. 4. Again, the MDI method located all damage with a false positive at one end of the supports. This has again proven that the method is viable in detecting localised damage accurately for up to three damage locations. However, the damage indicator did not reflect the severity of damage. It is, therefore, possible to deduce that damage indicator utilising statistical approach is working well in locating damage but not for evaluating the severity of damage. In the light of this, it is important as part of this study to propose a method to evaluate severity of damage in wood as presented in the following section.

Estimation of severity of damage

Damage cases discussed above were used in the estimation of severity of damage using Eq. (5). The severity of damage below zero percent is not meaningful, thus they were not shown. The results for single damage scenarios at location 2.25m are shown in Fig. 5 and the extent of damage is tabulated in Table 2. The damage evaluation algorithm captures the location of damage at position 2.25m very accurately, although there are some false positives. It estimated the severity of damage for severe damage with only 1% error. The predicted medium level of damage is reasonably good with 11% error. Nevertheless, the error for light damage has increased to 40%. The method has shown great potential in estimating severity of damage. It performs well in predicting the extent of damage from medium to severe single damage but with reduced accuracy for light damage cases, in addition to its ability to pin-point the exact location of damage. Any shortcomings of this method can be compensated by other NDT techniques which work well if damage location is generally known. It is also worth pointing out that in practice detecting the medium or severe damage when they occur is all that matters in order to avoid catastrophic failure.

The dual damage location cases 4 to 6 are presented in Fig. 6. The method identifies both damage at locations 2.25m and 3.375m. Even the light damage at position 3.375m which could not be identified using the damage localisation algorithm earlier, is located here. From Table 2, the predicted severe damage at 2.25m as well as at 3.375m is fairly accurate with errors of less than 5%, hence high confidence in using the method to evaluate severe damage. For the medium case, the method produces a 15% error in prediction, which still is considered quite acceptable in estimating severity of damage for wood considering inherent natural invariabilities in wood. However, for the light damage, the prediction is relatively poor but it still shows the location of damage.

With the success in detecting single and dual damage cases, it is of interest in this study to explore further the capabilities and limitations of the severity estimation using the proposed algorithm on tri damage scenarios. These damage cases (7 to 9) are illustrated in Fig. 7. It is obvious that all damage are being detected using the proposed method with a false positive at one of the supports. The error for light, medium and severe cases are ranging from 30~70%, 15~40% and 20~35%, respectively. The method can predict the severity of damage reasonably well when there are three damages existing in the structure. It is worth noting that as the number of damage locations increases, the predicted severity becomes smaller than simulated in magnitude. This may be due to the change in mode shape curvature being flat as more damage appears in the test sample. With the insight gained from this study, it is possible to overcome this shortcoming in the future by introducing a sensitivity function of counts and geometric location of damage into the severity estimation algorithm. This initial effort to estimate severity of damage in wood is believed to have advanced the knowledge of NDT for timber structures significantly.

Conclusions

A modified damage index method was proposed for detecting damage in timber beams using modal parameters obtained from experimental modal analysis. The new method aims to enhance the existing algorithm in detecting damage location, especially for multiple damage scenarios. It also provides an evaluation of damage severity on timber structures to fill a clear gap in knowledge in this area. The results showed that the proposed algorithm is effective and reliable in locating the damage even though it comes with some false positives. The algorithm is also capable of predicting the extent and severity of damage in terms of loss of moment of inertia for single and multiple damage scenarios.

Acknowledgements

The authors wish to thank the Centre for Built Infrastructure Research (CBIR), Faculty of Engineering, The University of Technology Sydney, for supporting this work. Within the Faculty of Engineering, The authors wish to also thank the staff of UTS Structures Laboratory for their assistance in conducting the experimental works.

References

1. Moody R (1994) Timber bridges-a rebirth. Woodland Management 15(4): 18-20
2. Thelandersson S, Larsen HJ (2003) Timber engineering. John Wiley and Sons Ltd, pp 15-22
3. Ross RJ, Pellerin RF (1994) Nondestructive testing for assessing wood members in structures-a review. Gen. Tech. Rep. FPL-GTR-70 (Rev.), Madison, WI, U.S., Department of Agriculture, Forest Service, Forest Products Laboratory, pp 1-40
4. Peterson ST, McLean DI, Symans MD, Pollock DG, Cofer WF, Emerson RN, Fridley KJ (2001) Application of dynamic system identification to timber beam: I. J Struct Eng 127 (4): 418-425.
5. ST Peterson ST, McLean DI, Symans MD, Pollock DG, Cofer WF, Emerson RN, Fridley KJ (2001) Application of dynamic system identification to timber beam: II. J Struct Eng 2001; 127 (4): 426-432.
6. Peterson ST, McLean DI, Pollock DG (2003) Application of dynamic system identification to timber bridges. J Struct Eng 129 (1): 116-124
7. Yang XY, Ishimaru Y, Iida I, Urakami H (2002) Application of modal analysis by transfer function to non-destructive testing of wood I: determination of localized defects in wood by the shape of the flexural vibration wave. J Wood Sci 48: 283-288
8. Yang XY, Ishimaru Y, Iida I, Urakami H (2002) Application of modal analysis by transfer function to non-destructive testing of wood II: modulus of elasticity evaluation of sections of differing quality in a wooden beam by the curvature of the flexural vibration wave. J Wood Sci 49: 140-144
9. Hu C, Afzal MT (2006) A statistical algorithm for comparing mode shapes of vibration testing before and after damage in timbers. J Wood Sci Online First

10. Hu C, Afzal MT (2006) A wavelet-based approach for damage localization in wood beams. J Wood Sci Online First

11. Kim J-T, Stubbs N (1995) Model-uncertainty impact and damage-detection accuracy in plate girder. J Struct Eng 121 (10): 1409-1417

Table 1. Inflicted damage scenarios

Damage Case	Scenario	Location per 8th of span length	Width, *w* (mm)	Depth, *h* (mm)	% loss of 'I'
1	4L	4	45	9	27.1
2	4M	4	45	27	65.7
3	4S	4	45	45	87.5
4	4S6L	4, 6	45	45, 9	87.5, 27.1
5	4S6M	4, 6	45	45, 27	87.5, 67.5
6	4S6S	4, 6	45	45, 45	87.5, 87.5
7	2L4L6L	2, 4, 6	45	All 9	All 27.1
8	2M4M6M	2, 4, 6	45	All 27	All 65.7
9	2S4S6S	2, 4, 6	45	All 45	All 87.5

Beam 1 for cases 1-6; Beam 2 for cases 7-9

Table 2. Estimation of severity of damage for single and multiple damage scenarios

Damage Case	Location(s) per 1/8th of span length	Simulated Damage (%)	Predicted Damage (%)
4L	4	27.1	15.6
4M	4	65.7	58.7
4S	4	87.5	88.6
4S6L	4	87.5, 27.1	87.0, 3.1
4S6M	4, 6	87.5, 65.7	91.3, 55.9
4S6S	4, 6	87.5, 87.5	88.8, 84.5
2L4L6L	6	All 27.1	19.7, 8.1, 17.3
2M4M6M	2, 4, 6	All 65.7	56.0, 37.5, 46.9
2S4S6S	2, 4, 6	All 87.5	68.1, 72.2, 58.2

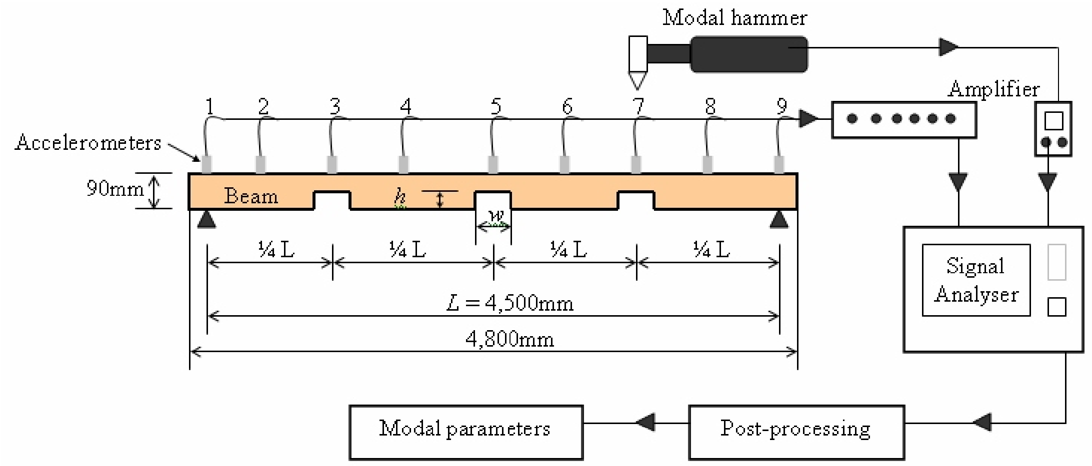

Fig. 1. Experimental modal analysis schematic diagram

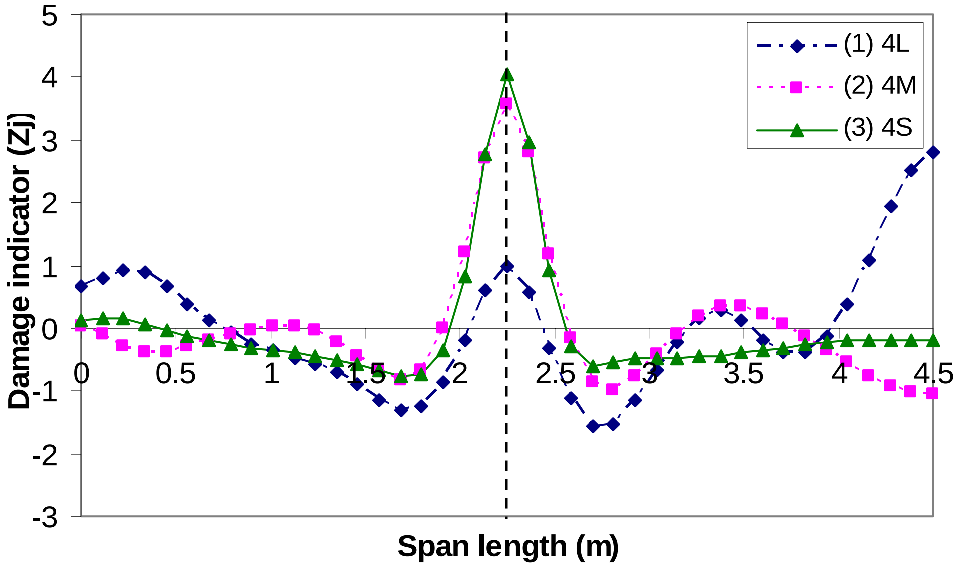

Fig. 2. Damage localisation for single damage cases 1 to 3

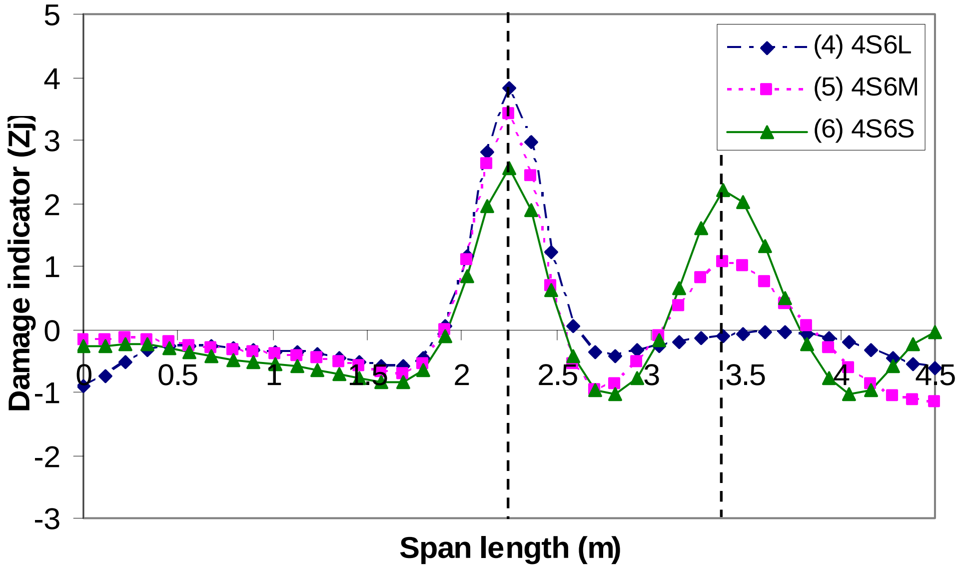

Fig. 3. Damage localisation for dual damage cases 4 to 6

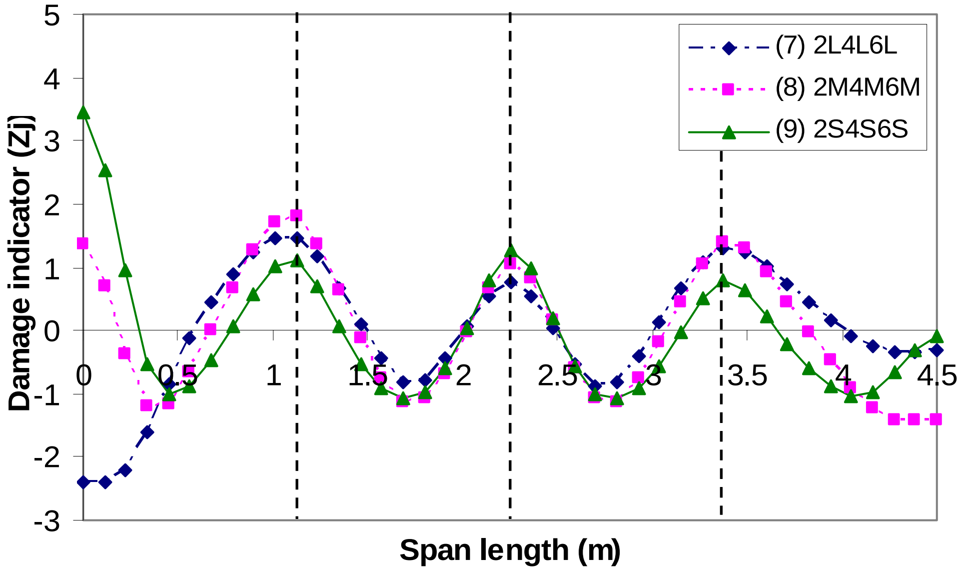

Fig. 4. Damage localisation for tri damage cases 7 to 9

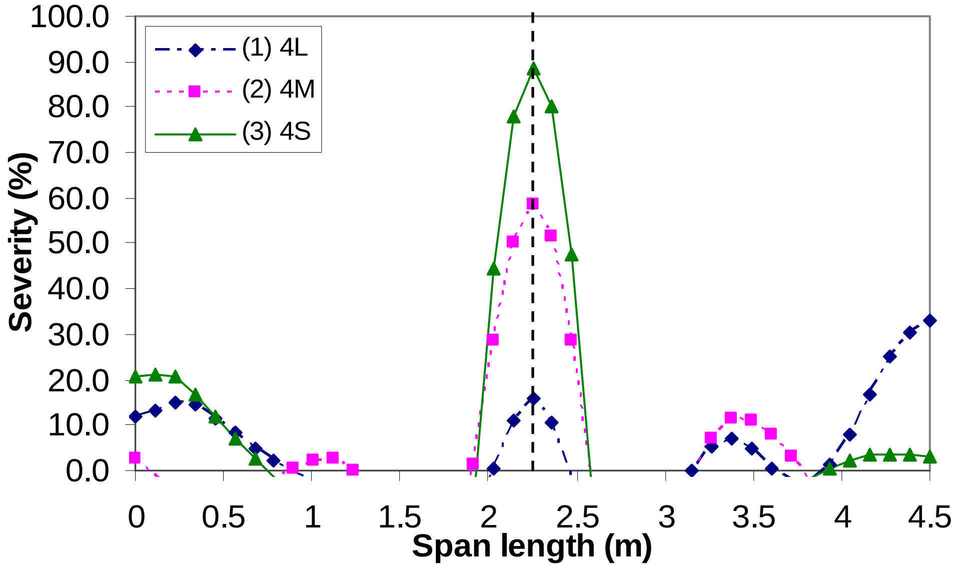

Fig. 5. Severity of damage for single damage cases 1 to 3

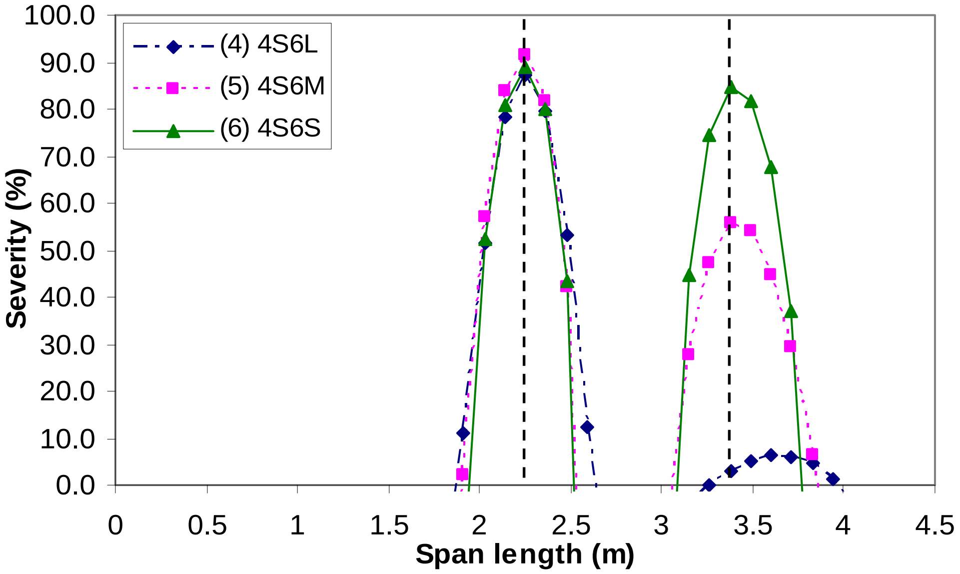

Fig. 6. Severity of damage for dual damage cases 4 to 6

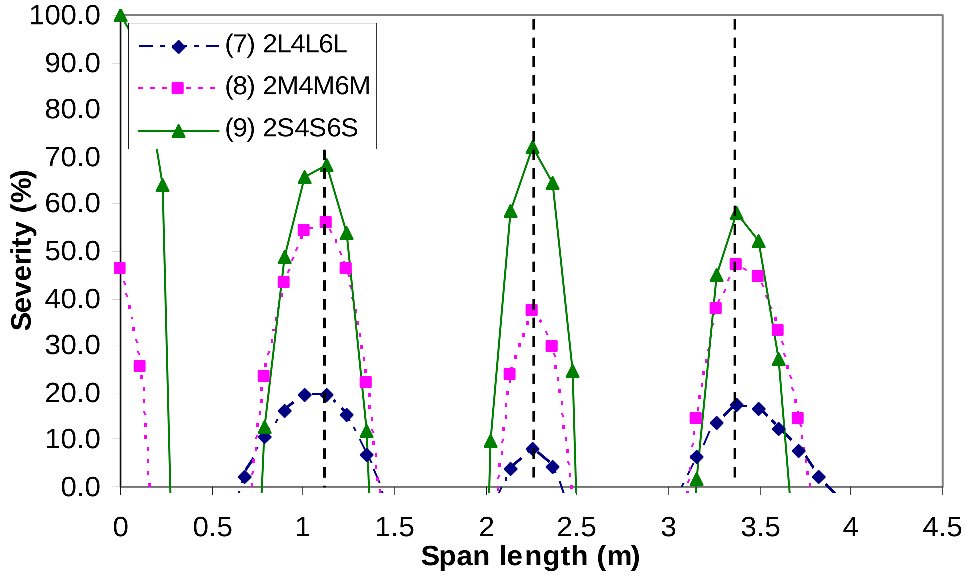

Fig. 7. Severity of damage for tri damage cases 7 to 9